Spatial Dynamics of Business Cycle Synchronization in Germany: A Grid-Based Distance Decay Analysis

Rouven Beiner

November 10, 2024

Contents

List of Figures

1 Introduction

A primary benefit of a gridded GDP dataset is its capacity to show how individual units interact to form aggregate outcomes, and how these outcomes, in turn, influence individual behaviors. This bottom-up approach enables the calculation of aggregate GDP in a new way, allowing for the estimation of confidence intervals around aggregate values—something not possible with a single aggregate GDP. From the perspective of complexity economics, this method is more reliable, as aggregate economic outcomes, such as prices or GDP, reflect the sum of individual transactions. More general, complexity asks "how individual elements react to the current pattern they mutually create, and what patterns, in turn, result" ([Arthur, 2021], p. 136). From my perspective, spatial raster data, as used in this study, provides a natural empirical counterpart to complex systems theory. While still an approximation of the underlying micro level data, it offers a finer level of detail than single aggregate values.

In this study I examine the spatial economic interdependency of german regions using 20x20km grid cells and the gdp per capita for each grid cell for the years 2000 to 2020. I analyze correlations in both the long term trend or growth path and interdependencies of short term fluctuations from the trend, i.e. the business cycle. The correlations of cells in proximity are estimated for different distances, allowing to calculate a distance decay curve for the regional trend and business cycle correlations. Multiple demographic variables on cell level are included as controls.

The results show that the business cycle is highly correlated with neighboring regions if the regions are nearby, but the correlation decreases with increasing distance. Interestingly for the business cycle, the correlation is only significant up to a distance of x km. For the trend i found that correlations are significant up to a much longer distance of x km. This result suggests that in the short run, regional gdp is only affected by neighboring regions, while in the long run, the regional GDP is also affected by regios far away. Apart from the contemporary correlations, i estimate the lagged correlations as well and found that for lagged business cycles of neighboring units correlate up to a wider radius than contemporary values. This result indicating, that the technology shocks from regions far away affect the respective region with a delay, just like a travel time.

The spillover effects of growth from one to another unit can be explained by mechanisms like bilateral trade and investment relationships or marshallian externalities such as knowledge spillovers and marked-based advantages.

To estimate distance decay effects, previous studies mostly used government regional (NUTS2) or sub regional (NUTS3) units. However this method is problematic for at least two reasons. First these units differ in size and to robustly separate the effect of the distance, the units must be adjusted by their size. Furthermore, the distance of a unit to another can not be consistently estimated, because of the size and shape of the units. Using grid cells of same sizes solve these problems.

2 Spillover effects and Marshallian externalities

Many empirical studies that analyzed growth correlations between neighboring countries indeed fount spillover effects. [Moreno and Trehan, 1997] considers the relationship between a country's growth rate and the economic growth of surrounding countries, finding evidence of spillovers across countries that are more closely. [Elhorst et al., 2024] investigates the distance decay effect and spatial reach of growth spillovers across 266 NUTS-2 EU regions from 2000 to 2018. Their findings show that the spatial reach varies between 700 and over 1500 km depending on the growth determinants.

When analyzing correlations of growth or productivity between different regions and considering the distance as and explanatory factor, the statitical findings should be grounded on an theoretic explanation. The distance is in fact not an economic explanation for spill over of business activity into neighboring regions, it is more like a proxy that correlates with several possible underlying mechanisms. However, data on the underlying mechanisms are usually harder to find than data on GDP and growth.

One underlying mechanism might be bilateral trade, and the amounth of trade between two units of course depends on their distance, their cultural proximity or trade unions. From a first sight, it is reasonable to expect that closer trade ties would result in more synchronized business cycles because stronger trade linkages create stronger demand and supply side spillovers across countries. Empirically this is confirmed by, among others, [Frankel and Rose, 1998] and [Clark and van Wincoop, 2001], who found that countries or regions with closer trade links tend to have more tightly correlated business cycles. However, there is an opposing effect of trade linkages on business cycle synchronization. According to classical Ricardian theory, increased trade leads to greater specialization ([Dornbusch et al., 1977]), which amplifies structural differences between economies and makes it less likely that sector-specific shocks in one economy will impact others. The specialization of the trading countries is a result of comparative cost advantages, which occur if different regions have different kinds of properties and therefore can specialize in different sectors. This is especially the case for regions with large distance, where differences in cultural, ecolological and other factors lead to different specializations. Since for this analysis units with small distances are analyzed, the causality chain of: trade ¿ different specialization ¿ growth decoupling does not hold. Therfore, correlations in growth between neighboring units can be for some extend explained by strong trade linkages and structural similarity or similar specializations. Another mechanism for growth spillover and business cycle synchronisation are financial linkages and foreign direct investments as found by [Dabla-Norris et al., 2010] and [Hsu et al., 2011].

Furthermore growth spillovers of regions located in proximity to each other can occur from various non-priced advantages or externalities initially proposed by Alfred Marshall ([Marshall, 1920]). Within the marshallian externalites, [Fujita et al., 1999] distinguishes further between knowledge spillovers as technological externalities and market-based advantages as pecuniary externalities. Pecuniary externalities can arise when firms in the same locality benefit from shared access to a specialized labor market or a network of input suppliers. For pecuniary externalities, Geographic proximity is particularly important ([Puga and Venables, 1996]). For example, it could be profitable for some suppliers to be located in a neighboring region of a saturated region with a lower degree of agglomeration, and still take advantage of proximity to that region. The role of technological interdependence or productivity shocks across regions and nations, measured usually by GDP per capita, is examined in classical endogenous growth models. In the famous Romer (1986) model, a firm's knowledge is a public good that any other firm can access at zero cost. In other words, once discovered, a piece of knowledge spills over instantly across the whole economy. In their model, [Chua, 1993] incorporating the weighted average of neighboring countries' physical capital and human capital in their growth models. The study provides evidence that countries can benefit from increased investment rates of its neighboring countries. Furthermore [Ertur and Koch, 2007] develops a growth model that quantifies the spatial externalities arising from technological stock in one country spilling over into neighboring countries, with spillover intensity diminishing with distance. In empirical studies like [Bottazzi and Peri, 2003] and [Funke and Niebuhr, 2005], R&D spillovers and the spatial reach of these effects on the regional level are analyzed. [Bottazzi and Peri, 2003] found that R&D spillovers are very localized and exist only within a distance of 300km. They highlight that while patents serve as a "public good"—widely accessible and internationally available—another component of the knowledge generated is linked to the experience of the scientists or "attached" to people. This localized knowledge primarily spreads through personal contacts and face-to-face interactions, effectively making it a "local public good". On regional level, [Rodríguez-Pose and Crescenzi, 2008] examines R&D investments, regional innovation systems, and socio-economic spillovers across the 25 European Union member countries. Their study emphasizes that economically productive knowledge diffusion is strongly influenced by proximity, with clear distance decay effects.

Marshallian externalities are one reason for the occurence of industry clusters within a region which can be described also statistically.

To summarize, correlations in growth and technological shocks, measured by the trend and the business cycle, between two neighboring units can be explained by their trade linkages, local knowledge spillovers, and market-based externalities such as a specialized labor market or a network of input supplies leading to similar sectoral specializations in both regions.

3 Data

I used the global gridded GDP dataset of [Wang and Sun, 2022] with fine spatial resolutions of 30 arc-seconds and 0.25 arc-degrees for the periods of 2000-2020 at 1-year intervals. They used the GRP for over 800 provinces (states) in 48 countries and downscaled these GRP by combining both Nighttime light images (NTL) and Gridded population datasets. Using NTL images alone for GRP downscaling are often biased because they underestimate urban centers and overestimate rural regions due to the saturation problem. Using population datasets assumes that GDP per capita is uniformly distributed within an administrative boundary. These problems can be mitigated to a certain extent when incorporating both NTL and population data. The GRP data used in their dataset is in germany on a NUTS-2 level, covering the 16 german states. To get the GDP per capita, I used the accurate global gridded population data from world pop, which is available for germany at a 1x1km scale for the years 2000-2020. I further included gridded demographic data from the 2011 German Census ([Statistisches Bundesamt, 2018]), with a spatial resolution of 100 meters, covering age and sex distribution for each cell. These census results, referenced to 9 May 2011, align well with the midpoint of the 2000-2020 analysis period. The data provides the count of persons within age groups: under 5, 10-19, 20-29, 30-39, 40-49, 50-59, 60-69, 70-79, and 80 and over, as well as male and female counts for each cell. I calculated the mean age and male share for each cell.

To achieve spatial consistency across the GDP, population, and demographic grids, all datasets (GDP,population,mean age, men share) were re-projected to the EPSG:3857 coordinate system using bilinear interpolation to maintain smooth transitions between cells. The GDP data was projected to a target resolution of 22.5 km x 22.5 km, closely reflecting the average cell size of the original 0.25-degree GDP grid in Germany. To align the population and demographic rasters with this resolution, both were resampled to match the 22.5x22.5 km grid cells, using "sum" for population and "average" for demographic data. Since the "sum" operation reduced population values for grid cells along Germany's borders, population data was extended beyond the border using the mean of the nearest available population data. In the population data, missing values within Germany's mainland borders, particularly occuring at lakes, were replaced with zeros (because the population on water is usually zero). The population grid, originally at 1 km x 1 km, was then resampled to match the 22.5 km GDP grid, so that both datasets share the same extent, cell size, and coordinate reference. This harmonization provides a stable basis for the estimation of GDP per capita per cell.

To construct a distance decay curve, the distances between any two cells must be precisely defined. Given that the cells are fixed and square in shape, the distance to the center of the nearest neighboring cell is exactly 22.5 km. To create a band of cells surrounding a specific cell that maintains consistent distances, a circular approximation is applied. Using only the n-th neighboring cells would lead to uneven real distances, as diagonal distances are inherently larger than horizontal or vertical ones. For each target radius r, a distance corridor is defined as

$$\mathrm{r} - 0.5 \leq \mathrm{distance} \leq \mathrm{r} + 0.5,$$

where the distance from the origin cell (x, y) to the other cell (i, j) is calculated as

$$\mathrm{distance} = \sqrt{(x - i)^2 + (y - j)^2}.$$

Figure 1 illustrates how cells at different distances are selected. The cell pairs that match specific distances are stored.

As the distance between grid cells increases, the total number of cell pairs at each distance also grows. For instance, while each cell has only 8 neighboring cells at a distance of 1, it has 12 at a distance of 2, leading to a significantly higher count of cell pairs separated by greater distances. Table **??** lists the total number of grid-cell pairs across Germany at each specified distance.

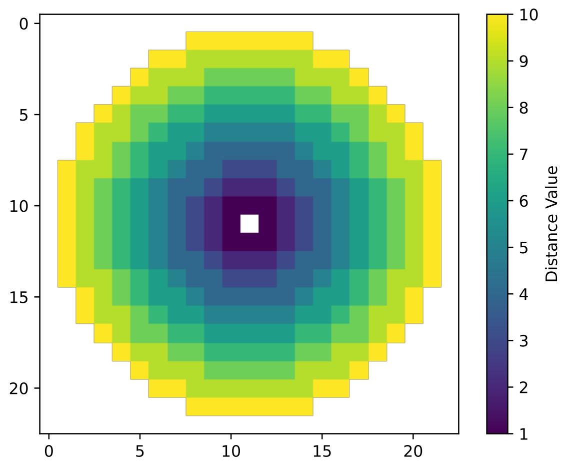

Figure 1: Cell distances

Illustration of cell selection for different distances from a central cell.

Distance	**Number of Cell Pairs**
1	7606
2	11036
3	14296
4	27631

Table 1: Number of Cell Pairs by Distance

4 Time series preparation

To extract the business cycle and trend, I applied the Hodrick-Prescott filter as introduced by [Hodrick and Prescott, 1997]. The trend component is obtained directly by applying the HP filter once. The business cycle component is extracted from the target variable (GDP or GDP per capita) using a bandpass filtering procedure. The Bandpass filtering is done with the Hodrick-Prescott (HP) filter which is applied twice to the time series to extract the business cycle frequency component, as proposed by [Pedersen, 2001]. First, the HP high-pass filter with $\lambda_1 = 2413.06$ removes the long-term trend, i.e. the trend of the filter is subtracted from the raw time series. Then, the HP low-pass filter with $\lambda_2 = 2.91$ is applied to the detrended series, i.e. the cycle of the filter is subtracted from the detrended series to get the final business cycle component. The HP filter minimizes the following objective function:

$$\min_{\{\tilde{y}_t\}_{t=1}^{T}} \left\{ \sum_{t=1}^{T} (y_t - \tilde{y}_t)^2 + \lambda \sum_{t=2}^{T-1} [(\tilde{y}_{t+1} - \tilde{y}_t) - (\tilde{y}_t - \tilde{y}_{t-1})]^2 \right\}$$

The filter computes a stochastic trend $\{\tilde{y}_t\}_{t=1}^{T}$ by minimizing the squared deviations from the trend $(y_t - \tilde{y}_t)^2$, constrained to keep the squared second differences small $[(\tilde{y}_{t+1} - \tilde{y}_t) - (\tilde{y}_t - \tilde{y}_{t-1})]^2$.

The frequency response function of the Hodrick-Prescott filter is given by:

$$R(\omega) = \frac{1}{1 + 4\lambda[1 - \cos(\omega)]^2}$$

Now solving for the HP-filter parameter λ:

$$\lambda = \frac{1 - R(\omega)}{4R(\omega)[1 - \cos(\omega)]^2}$$

It can be shown that in the case of the HP filter, the gain function equals the frequency response function. Using a gain of $R(\omega) = 0.5$ and replacing the frequency in radians (ω) with the ordinary frequency (f) multiplied by 2π, the equation can be simplified as follows:

$$\lambda = \frac{1 - 0.5}{4 \cdot 0.5 \cdot [1 - \cos(\omega)]^2} = \frac{0.25}{[1 - \cos(\omega)]^2} = \frac{0.25}{[1 - \cos(2\pi f)]^2}$$

The lambda parameters are set so that the frequency cut-off occurs at frequencies higher than 2 years and lower than 12 years. These cut-offs are based on the U.S. recession durations reported by the NBER, where all recessions from 1858 onwards last longer than 17 months and shorter than 146 months ([National Bureau of Economic Research, 2024]) Therefore, the corresponding ordinary frequencies of $f_1 = 1/12$ and $f_2 = 1/2$ are used:

$$\lambda_1 = \frac{0.25}{\left(1 - \cos\left(\frac{1}{12} 2\pi\right)\right)^2} = 13.93$$

$$\lambda_2 = \frac{0.25}{\left(1 - \cos\left(\frac{1}{2} 2\pi\right)\right)^2} = 0.063$$

The HP filter is widely used because of its advantegous properties such as the ability to generate stationary time series when time series integrated up to order four ([King and Rebelo, 1993]), or of course the symmetry of the filter, such that no phase shift is introduced. In fact, as shown by [Pedersen, 2001] the HP filter is an close approximation to an ideal high-pass filter, which is a filter which sharply cuts off components at frequencies below and above the bandpass cutoffs. However there are some drawbacks of the HP filter as clearly shown by [Hamilton, 2017]. Especially the the fact that Filtered values at both ends of the sample are very different from those in the middle because the HP filter is an infinite dimensional moving average filter in the time domain, allpied to non infinite time series. Therefore, some authors even advise to cut of the first and last observations to minimize the problem ([Baxter and King, 1999]). Of course this is not an option for small size time series as in this analysis. Furthermore especially the last observations are in most scenarios of highest interest, and removing them would reduce the worth of the analysis.

To reduce endpoint bias, I propose a three-step approach. First, forecasts are generated for both ends of the time series (a backcast for the beginning and a forecast for the end). Second, the HP filter is applied to this extended series. Finally, the forecasted values are trimmed to restore the original series length.

To evaluate this method, I generated 1,000 synthetic time series, each modeled as a random walk with drift and an error term following an AR(10) process:

$$Y_t = Y_{t-1} + \sum_{j=1}^{10} \phi_j \epsilon_{t-j} + \delta + \epsilon_t, \tag{1}$$

where $\delta \sim N(0,1)$ is the drift term, $\phi_j \sim N(0,0.2)$ are the AR(10) parameters, and $\epsilon_t \sim N(0,1)$ are the error terms.

Each series Y_i was then reduced to a 100-point middle segment y_i. An ARIMA(10,1,0) model was fitted to this middle segment y_i to forecast the next 10 values. For the backcast, y_i was reversed, fitted with an ARIMA(10,1,0), and then forecasted; the forecast was reversed back to its original order and added to the beginning of y_i.

An HP filter was applied to both the extended y_i^* (backcasted and forecasted) series and the middle segment y_i alone. Errors were assessed by comparing the HP filter cycle components of both the y_i^* and y_i against the cycle derived from the full series Y_i. Figure 2 shows the resulting distributions of the absolute errors, including the 5th and 95th percentiles, for both methods. The effectiveness of this method in reducing the HP filter's endpoint bias naturally depends on the predictability of the series. In the simulation, the mean error over all 100 time points for the standard method was 0.1578, whereas the mean error for the extended method was 0.1395. This represents an error reduction of 11.6%.

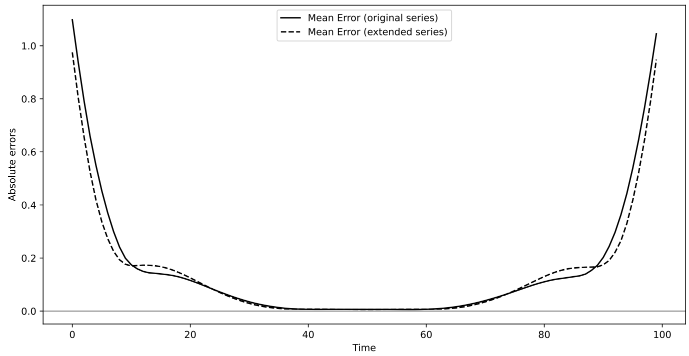

Figure 2: Hodrick-Prescott endpoint error simulation

This figure shows the absolute error of the unadjusted HP-filter cycle and the adjusted (using back- and forecasting).

5 Descriptive Statistics

I aggregated the GDP of all German grid cells into a total GDP using simple summation. To construct 5% and 95% confidence intervals over the entire time range, I applied a bootstrap method with 25,000 samples. The aggregate GDP and its confidence intervals were then decomposed into cycle and trend components, with the cycle derived using the HP bandpass filter and the trend via the standard HP filter. Figure 3 displays all three resulting time series.

Figure 5 shows the distributions of GDP, population, and GDP per capita, averaged annually over the period 2000–2020. Values are displayed on a logarithmic scale for clearer visualization.

Clusters appear in and around large cities, where higher GDP per capita values are observed, likely due to firms locating production or logistics facilities on the urban outskirts, where lower population density positively affects GDP per capita.

Figure 5 presents the mean age and male share, averaged across each grid cell for the period 2000–2020.

A noticeable age disparity exists between the former East and West German regions, with East German areas tending toward an older population. Additionally, the male share is notably higher in the northeastern region, particularly around Schleswig-Holstein.

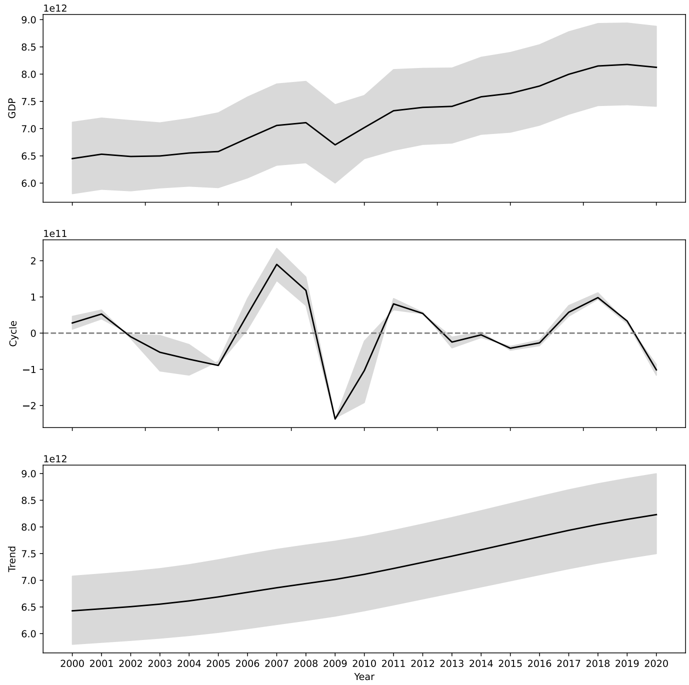

Figure 3: Aggregate GDP and Components

Aggregate GDP (first), cycle component (second), and trend component (third) over time along with 5% and 95% quantiles.

6 Correlation Analysis

In the first step, correlations between grid cells at varying distances are estimated in a baseline model, where the correlation coefficient serves as the dependent variable and distance indicators, representing spatial proximity between cells, are the only independent variables.

Two separate OLS models are estimated: one for the business cycle correlation and another for the trend correlation. The model summaries are presented in Table X, and the distance decay curve, showing distance coefficients with 95% confidence intervals, is displayed in Figure 6. The results indicate that both business cycle and trend correlations are higher for closer regions and decrease monotonically with increasing distance. However, the rate of decline diminishes with distance. Trend correlations are generally

Figure 4: Rasterized and EPSG:3857 projected grid cells over Germany, displaying GDP, population, and GDP per capita.

higher than cycle correlations but exhibit slightly wider (though still narrow) confidence intervals. In this basic OLS model without additional controls, the coefficients represent the average correlations for each distance.

A second model is estimated for both cycle and trend correlations, incorporating additional control variables. The independent variables include distance indicators, the average population, average male share, and average age across both regions, as well as the absolute difference in population between the regions. As with the baseline model, this approach captures contemporary effects and assumes symmetric causality, as it does not differentiate the direction of causality. The absolute population difference serves as the sole possible indicator of directional influence, suggesting that more densely populated regions may impact neighboring, less densely populated areas. Figure 7 shows the distance decay curve for the second model, with the corresponding regression results summarized in Table X. The curve displays a similar pattern, with correlations decreasing monotonically with distance. However, the inclusion of control variables shifts the levels of the coefficients; negative coefficients for larger distances do not imply negative correlations, but rather adjusted lower levels relative to the baseline. Confidence intervals are wider in this model, which calls for cautious interpretation. In large samples, even small effect sizes can become statistically significant due to the reduced standard error (SE) as sample size (N) increases, leading to higher t-statistics and lower p-values, thus more easily rejecting the null hypothesis. The trend correlations are not well-explained by distance alone, as indicated

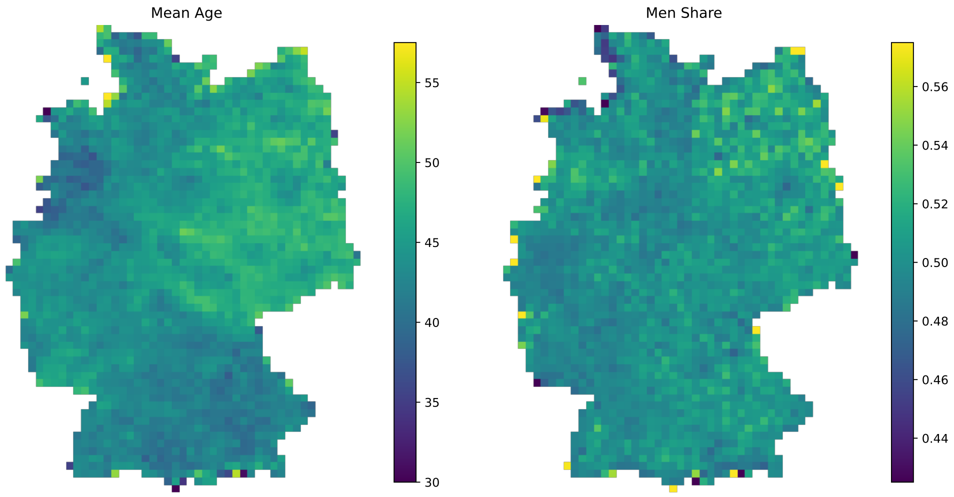

Figure 5: Demographic Patterns Across Germany

Rasterized and EPSG:3857 projected grid cells over Germany, displaying demographic characteristics.

by the low R-squared in the baseline model for trend correlation. This suggests that long-term regional GDP is less influenced by neighboring regions' GDP and more by other structural factors, some of which are captured by the demographic variables included in the extended model.

References

[Arthur, 2021] Arthur, W. B. (2021). Foundations of complexity economics. *Nature Reviews Physics*, 3(2):136–145.

[Baxter and King, 1999] Baxter, M. and King, R. G. (1999). Measuring Business Cycles: Approximate Band-Pass Filters for Economic Time Series. *The Review of Economics and Statistics*, 81(4):575–593.

[Bottazzi and Peri, 2003] Bottazzi, L. and Peri, G. (2003). Innovation and spillovers in regions: Evidence from european patent data. *European Economic Review*, 47(4):687–710.

[Chua, 1993] Chua, H. (1993). Regional spillovers and economic growth. Harvard University, unpublished.

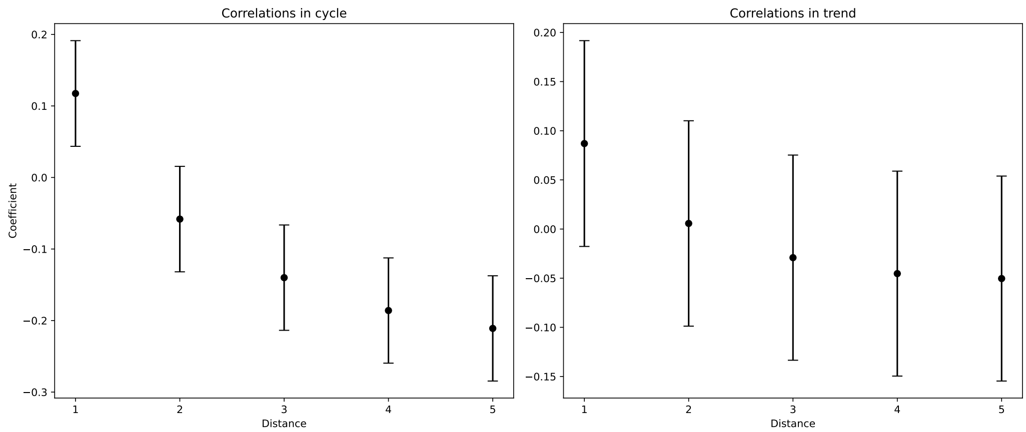

Figure 6: Baseline Model: Distance Decay Curve with 95% Confidence Intervals

[Clark and van Wincoop, 2001] Clark, T. E. and van Wincoop, E. (2001). Borders and business cycles. *Journal of International Economics*, 55(1):59–85. Intranational & International Economics.

[Dabla-Norris et al., 2010] Dabla-Norris, E., Honda, J., Lahreche, A., and Verdier, G. (2010). Fdi flows to low-income countries: Global drivers and growth implications. IMF Working Paper WP/10/132, International Monetary Fund. Strategy, Policy, and Review and African Departments.

[Dornbusch et al., 1977] Dornbusch, R., Fischer, S., and Samuelson, P. A. (1977). Comparative advantage, trade, and payments in a ricardian model with a continuum of goods. *The American Economic Review*, 67(5):823–839.

[Elhorst et al., 2024] Elhorst, J. P., Tziolas, I., Tan, C., and Milionis, P. (2024). The distance decay effect and spatial reach of spillovers. *Journal of Geographical Systems*, 26(2):265–289.

[Ertur and Koch, 2007] Ertur, C. and Koch, W. (2007). Growth, technological interdependence and spatial externalities: theory and evidence. *Journal of Applied Econometrics*, 22(6):1033–1062.

[Frankel and Rose, 1998] Frankel, J. A. and Rose, A. K. (1998). The endogenity of the optimum currency area criteria. *The Economic Journal*, 108(449):1009–1025.

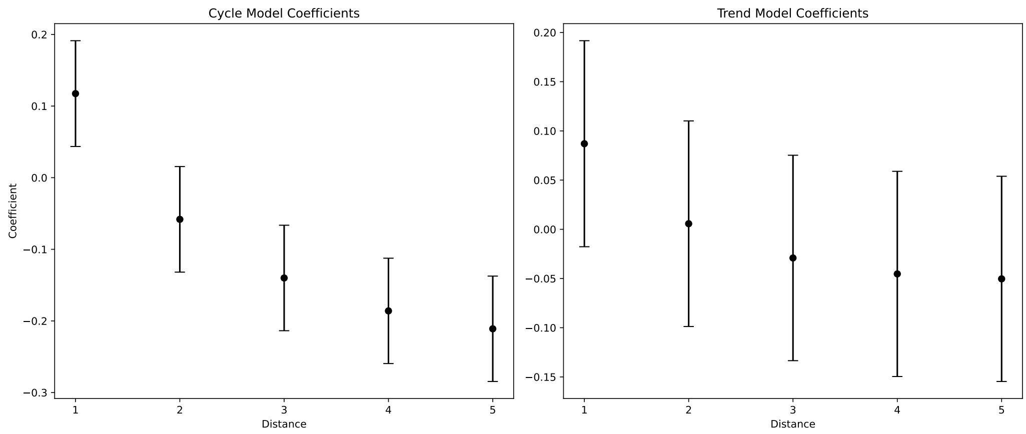

Figure 7: Control Model: Distance Decay Curve with 95% Confidence Intervals

[Fujita et al., 1999] Fujita, M., Krugman, P., and Venables, A. (1999). *The Spatial Economy: Cities, Regions, and International Trade*. MIT Press, Cambridge, MA.

[Funke and Niebuhr, 2005] Funke, M. and Niebuhr, A. (2005). Regional geographic research and development spillovers and economic growth: Evidence from west germany. *Regional Studies*, 39(1):143–153.

[Hamilton, 2017] Hamilton, J. D. (2017). Why you should never use the hodrick-prescott filter. Working Paper 23429, National Bureau of Economic Research, Cambridge, MA.

[Hodrick and Prescott, 1997] Hodrick, R. J. and Prescott, E. C. (1997). Postwar u.s. business cycles: An empirical investigation. *Journal of Money, Credit and Banking*, 29(1):1–16.

[Hsu et al., 2011] Hsu, C.-C., Wu, J.-Y., and Yau, R. (2011). Foreign direct investment and business cycle co-movements: The panel data evidence. *Journal of Macroeconomics*, 33(4):770–783.

[King and Rebelo, 1993] King, R. G. and Rebelo, S. T. (1993). Low frequency filtering and real business cycles. *Journal of Economic Dynamics and Control*, 17(1):207–231.

[Marshall, 1920] Marshall, A. (1920). *Principles of Economics*. Macmillan, London.

Table 2: Regression Results for Cycle Correlations

Dependend:	Cycle corr	Cycle corr
Distance 1	0.7320***	0.1174**
	(0.003)	(0.038)
Distance 2	0.5463***	-0.0582
	(0.003)	(0.038)
Distance 3	0.4600***	-0.1400***
	(0.002)	(0.038)
Distance 4	0.4112***	-0.1860***
	(0.002)	(0.038)
Distance 5	0.3846***	-0.2110***
	(0.002)	(0.038)
Mean Population	-	1.622e-07***
		(4.02e-08)
Population Difference	-	-1.095e-06***
		(2.67e-08)
Mean Men Share	-	0.6302***
		(0.064)
Mean Age	-	0.0072***
		(0.000)
Observations	83,959	83,959
R-squared	0.103	0.166
Adjusted R-squared	0.103	0.166
F-statistic	2418.0	2087.0

Notes: * p<0.05, ** p<0.01, *** p<0.001

[Moreno and Trehan, 1997] Moreno, R. and Trehan, B. (1997). Location and the growth of nations. *Journal of Economic Growth*, 2:399–418.

[National Bureau of Economic Research, 2024] National Bureau of Economic Research (2024). U.s. business cycle expansions and contractions. Accessed: 2024-08-08.

[Pedersen, 2001] Pedersen, T. M. (2001). The hodrick–prescott filter, the slutzky effect, and the distortionary effect of filters. *Journal of Economic Dynamics and Control*, 25(8):1081–1101.

[Puga and Venables, 1996] Puga, D. and Venables, A. (1996). The spread of industry: Spatial agglomeration in economic development. *Journal of the Japanese and International Economies*, 10:440–464.

Table 3: Regression Results for Trend Correlations

Dependend:	Trend corr.	Trend corr.
Distance 1	0.8401***	0.0870
	(0.005)	(0.053)
Distance 2	0.7463***	0.0057
	(0.004)	(0.053)
Distance 3	0.7063***	-0.0291
	(0.003)	(0.053)
Distance 4	0.6868***	-0.0453
	(0.002)	(0.053)
Distance 5	0.6798***	-0.0504
	(0.003)	(0.053)
Mean Population	-	2.793e-07***
		(5.7e-08)
Population Difference	-	-1.342e-06***
		(3.78e-08)
Mean Men Share	-	0.0516
		(0.091)
Mean Age	-	0.0169***
		(0.001)
Observations	83,959	83,959
R-squared	0.012	0.066
Adjusted R-squared	0.012	0.066
F-statistic	260.8	739.4

Notes: * $p<0.05$, ** $p<0.01$, *** $p<0.001$

[Rodríguez-Pose and Crescenzi, 2008] Rodríguez-Pose, A. and Crescenzi, R. (2008). Research and development, spillovers, innovation systems, and the genesis of regional growth in europe. *Regional Studies*, 42(1):51–67.

[Statistisches Bundesamt, 2018] Statistisches Bundesamt (2018). Grid Cells Results of the 2011 Census: Age and Sex Distribution. Federal Statistical Office of Germany, Wiesbaden. More information is available at www.zensus2011.de. © Statistisches Bundesamt, Wiesbaden 2018.

[Wang and Sun, 2022] Wang, T. and Sun, F. (2022). Global gridded gdp data set consistent with the shared socioeconomic pathways. *Scientific Data*, 9(1):221.